Available online at www.sciencedirect.com
SCIENCE DIRECT®
ELSEVIER
International Journal of Solids and Structures 43 (2006) 1061–1078
INTERNATIONAL JOURNAL OF SOLIDS and STRUCTURES
www.elsevier.com/locate/ijsolstr

The effect of cell irregularity on the high strain compression of 2D Voronoi honeycombs

H.X. Zhu *, S.M. Thorpe, A.H. Windle

Department of Materials Science and Metallurgy, Cambridge University, Pembroke Street, Cambridge CB2 3QZ, UK

Received 29 October 2004; received in revised form 6 May 2005
Available online 28 June 2005

Abstract

The in-plane compression of low-density irregular Voronoi honeycombs with periodic boundary conditions has been simulated to engineering strains of 0.6 using finite element analysis. Different degrees of geometric irregularity in the honeycomb cells, as quantified using a regularity parameter, have been employed. The stress–strain predictions reveal that, for a fixed relative density, a more irregular honeycomb has a higher tangential modulus at low strain but supports a lower compressive stress at higher strain (above approximately 0.04) when compared with a more regular honeycomb. A combined 'springs in parallel' and 'springs in series' model has also been compared quantitatively with the simulation stress–strain results, the relative importance of the 'springs in series' mechanism having been found to increase with the irregularity of the honeycomb and, in many cases, with the applied compressive strain. In addition, the dependency of the Poisson's ratio, the maximum bending strain in the cell walls, and the mean junction rotation upon the applied compressive strain have also been determined for a range of honeycomb irregularities.

Keywords: Voronoi; Honeycomb; High-strain compression; Buckling; Stress–strain

1. Introduction

Honeycombs are effectively 'two-dimensional' cellular structures, being comprised of prismatic, rather than polyhedral, cells. Both man-made and natural honeycombs are used in a broad range of engineering applications, and represent an important class of material (an extensive review may be found in Gibson and Ashby, 1997). One property of honeycombs often utilised in packaging or protective materials is their

* Corresponding author. Present Address: School of Engineering, Cardiff University, Cardiff CF24 3AA, UK. Tel.: +0044 029 20874824; fax: +0044 029 20874716.
E-mail address: zhuh3@cf.ac.uk (H.X. Zhu).

0020-7683/$ - see front matter
doi:10.1016/j.ijsolstr.2005.05.008

excellent capacity for energy absorption under high compressive strain. The in-plane compression of regular honeycomb structures has been studied by many, including the initial work by Abd El-Sayed et al. (1979) and Gibson et al. (1982) and the later developments by Warren and Kraynik (1987), Papka and Kyriakides (1994), Masters and Evans (1996), and Zhu and Mills (2000). Such regular structure analyses do not, however, account for natural variations in microstructure of real honeycombs, nor provide a strong basis for the study of (disordered) three-dimensional foam materials. Several studies which model irregular honeycombs using two-dimensional Voronoi diagrams have been carried out (Silva et al., 1995; Silva and Gibson, 1997; Chen et al., 1999; Zhu et al., 2001a), although are confined to relatively low compressive strains. The aim of this study is to extend previous low-strain work (Zhu et al., 2001a), in order to determine the influence of introducing varying degrees of geometrical irregularity to elastomeric Voronoi honeycombs on their in-plane mechanical properties at high compressive strains.

2. The Voronoi honeycomb structures

2.1. Generating the periodic structure

A cellular solid may be formed by the nucleation and growth of cells. If all cells nucleate simultaneously in space and grow at a single isotropic rate, then the resulting structure is described by a Voronoi diagram. To model the structure of irregular honeycombs, we use Voronoi diagrams with varying degrees of regularity (as defined in the following section). To create the Voronoi structures, n points are firstly generated in a central square with area a_0 and periodic boundary conditions using software developed for this study; each point is a nucleus, or 'seed', for a single Voronoi cell. Taking a Cartesian coordinate system, seeds are placed in the square by deriving x and y coordinates independently from pseudo-random numbers[1] generated between zero and one. Once the first seed is placed, subsequent candidates are accepted only if they are located no nearer than a minimum allowed distance δ from all other seeds; that is, if discs of equal diameter δ centred on the seeds do not overlap. To maintain periodic boundary conditions, each seed is also copied into the surrounding 8 equivalent squares and the process is repeated until n seeds have been specified. If the value of δ, and hence the diameter of the discs, is set to zero, then the seeds are distributed randomly in space. Once all seeds have been specified, the Voronoi cell for each seed may be obtained by constructing the perpendicular bisectors of the lines connecting this seed to every other; the required cell around the seed being the smallest which is bounded by the bisectors, and which therefore delineates the region closer to the contained seed than any other. In practice, there are typically a proportionately small number of neighbouring seeds which yield bisectors bounding the cell. The Voronoi cells are generated using software developed for this study, and periodic boundary conditions are maintained at the edges of the square throughout.

2.2. Quantifying the honeycomb regularity

A regular hexagonal honeycomb, composed of identical cells each having six sides and vertex angles of 120°, is a fully ordered 2D Voronoi honeycomb. In order to fit n hexagonal cells into an area a_0, the distance d_0 between each seed and its 6 nearest neighbours must be equal to:

$$d_0 = \left(\frac{2a_0}{n(3)^{1/2}}\right)^{1/2} \tag{1}$$

[1] The 'rand( )' library function on the Silicon Graphics IRIX 6.5 platform has been used here.

To construct a *random* Voronoi honeycomb with n cells in the area a_0, and hence to randomly place n identical discs in the area a_0, then the minimum exclusion distance, δ, between the seeds (alternatively, the diameter of the hard discs) must be less than d_0; otherwise, it will be impossible to incorporate n cells. The value of d_0 is therefore an upper limit on the diameter of the n identical hard discs which may be accommodated. In order to quantify the regularity of the Voronoi honeycomb structures, we define a parameter, α, as follows:

$$\alpha = \frac{\delta}{d_0} \tag{2}$$

where $\alpha = 1$ (i.e. $\delta = d_0$) for a regular hexagonal honeycomb. For a fully-random (Poisson Voronoi) structure, $\alpha = 0$ ($\delta = 0$). The statistical distributions of a range of properties of 2D Voronoi honeycombs have been derived by Zhu et al. (2001b) in terms of α. By comparison, the disc packing density is given by ($\delta^2 n\pi/4a_0$) in the above notation. When α is zero, the packing density is also zero; when $\alpha = 1$, however, the value of the packing density is $(\pi/2(3)^{1/2})$, or 0.9069.

3. Computational methods and results

3.1. General methodology

The mechanical properties of the Voronoi honeycombs described in this paper have been determined using the ABAQUS finite element analysis (FEA) software. Each cell wall was modelled using 1–5 'Timoshenko' beam elements (B22 type ABAQUS elements), the number of elements depending upon the cell wall length. The cell walls were prescribed to be of equal and uniform thickness, t, so that the relative density, ρ, of each Voronoi honeycomb is given by

$$\rho = \frac{t\sum_{i=1}^{N} l_i}{a_0} \tag{3}$$

where l_i are the individual cell wall lengths, N is the total number of cell walls and a_0 is the area of the square model (an example honeycomb is shown in Fig. 1a). In this paper, unless otherwise stated, Voronoi honeycombs with a relative density of 0.01 were used, which was achieved by setting the value of t appropriately. The Young's modulus of the cell walls, E_s, was set to 10^8, and their Poisson's ratio was set to 0.3. The solid material of the cell walls was treated as behaving linear elastically throughout, and the option to apply 'Riks' method' was selected.

Strain was applied incrementally to each model by imposing displacements upon a set of parallel boundaries, in order to simulate uniaxial compression; the periodic nature of the boundary conditions being described below. In many cases, it was found that a strain of 0.6 could not be reached before a failure to converge upon a solution by the FEA software was encountered. Consequently, in order to achieve between 10 and 20 results for each set of model parameters, it was necessary to run between 20 and 60 FEA simulations on different honeycomb structures. The results presented represent, unless otherwise stated, an average over the 10–20 successful runs.

3.2. The periodic boundary conditions

As demonstrated previously (Zhu et al., 2001a), the low-strain Young's modulus of a honeycomb may be underestimated if periodic boundary conditions are not used. Therefore, as in the aforementioned low-strain study, periodic boundary conditions have been used here, so that the Voronoi honeycomb model

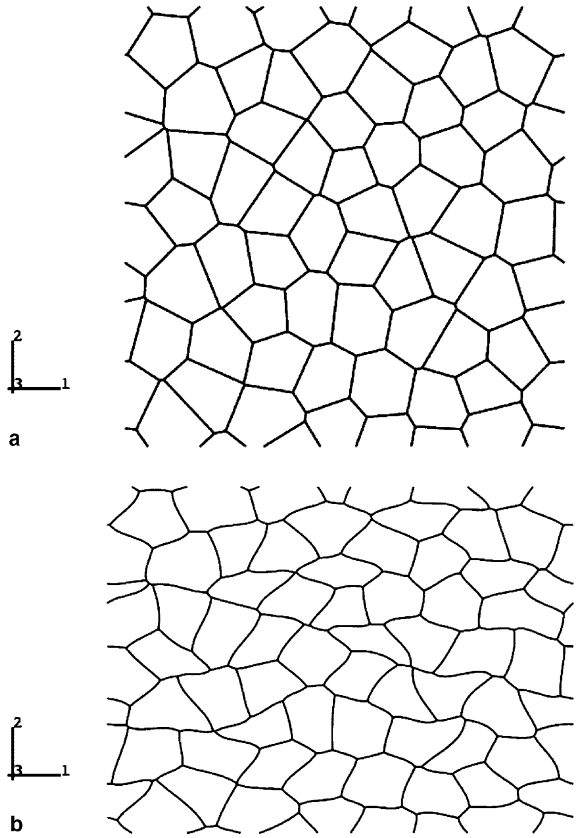

Fig. 1. A model periodic Voronoi honeycomb structure ($\alpha = 0.7$, $n = 64$). The honeycomb is shown (a) in its undeformed state; and (b) under uniaxial compressive strain.

structure is treated as the 'unit cell' of an infinite periodic honeycomb (see Fig. 1a). When the honeycomb model is placed under strain, the periodic boundary conditions dictate that corresponding nodes on the opposite edges of the unit cell have coupled displacements and identical orientations (see Fig. 1b).

3.3. The size of the honeycomb unit cell

In order to simplify the results, the stresses are reduced by dividing by ρ^3 and by the Young's modulus E_s of the solid material of the honeycomb; this is dimensionally correct, for a given honeycomb geometry, provided that the dominant deformation mechanism is bending (ρ is low). The reduced stress is therefore given by

$$\bar{\sigma} = \frac{\sigma}{E_s \rho^3} \tag{4}$$

Because the solid material is assumed to be elastic throughout the deformation, the adoption of 'reduced stress' in Eq. (4) can eliminate the effect of the honeycomb relative density and the Young's modulus of the solid material and make the results more useful.

The sensitivity of the results to the number of cells, n, in the honeycomb unit cell was examined by comparing the predicted stress–strain results for unit cells with $n = 64$, 144, and 225 using a fixed value of

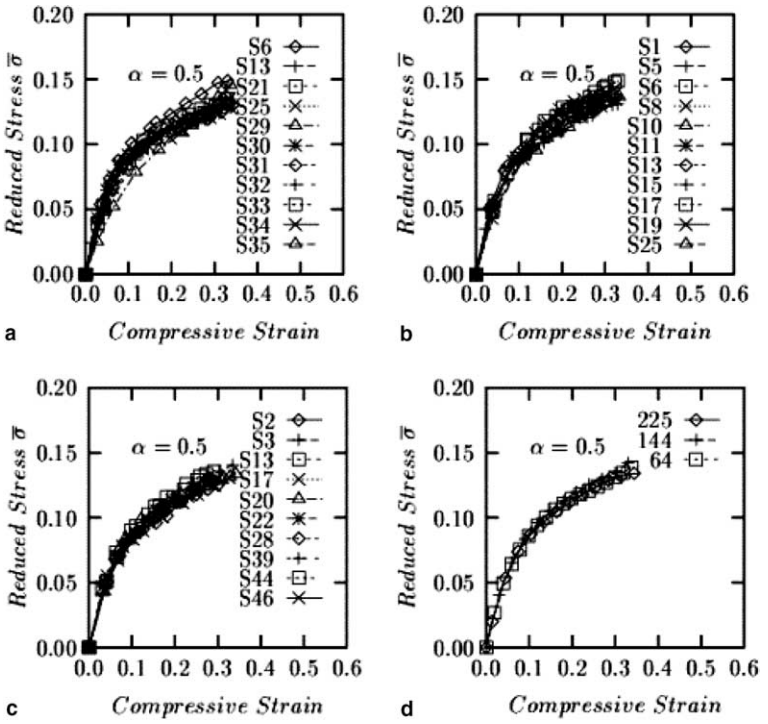

Fig. 2. The influence of the number of cells, n, in the honeycomb 'unit cell' on the reduced compressive stress–strain (FEA) predictions for model structures with $\alpha = 0.5$. Results are shown for: (a) $n = 64$; (b) $n = 144$; (c) $n = 225$. (d) The mean results compared for $n = 64$, 144 and 225.

$\alpha = 0.5$. For each value of n, 20–60 different Voronoi honeycombs were generated to ensure that 10–20 successful FEA runs were obtained. In each case, the relative density was set to 0.01 by adjusting the cell wall thicknesses. The predictions for the reduced compressive stress (see Eq. (4)) are plotted against compressive strain for each value of n in Fig. 2a–c, respectively, and the mean results for each value of n are compared in Fig. 2d. From Fig. 2d it can be seen that the mean predicted stress–strain relationship varies little with the changes to n, while the plots in Fig. 2a–c show that there is a greater variation between individual results for a given value of n as the value of n decreases. When $n = 64$, the deviations between samples are nonetheless reasonably small and hence, in order to manage the computational time required for the FEA analysis, the size of the unit cell was fixed at 64 cells.

3.4. Isotropic properties

In Fig. 3a, the (mean) FEA predictions for the reduced compressive stress (see Eq. (4)) are shown as a function of the applied compressive strain for Voronoi honeycombs with $\alpha = 0.7$ and a relative density of 0.01. The results are shown for compression along the two orthogonal directions labelled the x- and y-axes when generating the 'seeds' for the Voronoi cells. For clarity, the standard deviations are shown for results in the x-direction only and these are seen to be relatively small by comparison with the predicted stress values. In Fig. 3b the corresponding mean Poisson's ratio results (defined as the ratio of the laterally-induced strain to the directly-applied strain) are shown; where v_{xy} represents the Poisson's ratio for applied compression in the x-direction, and v_{yx} that for compression in the y-direction. Again, the standard deviations

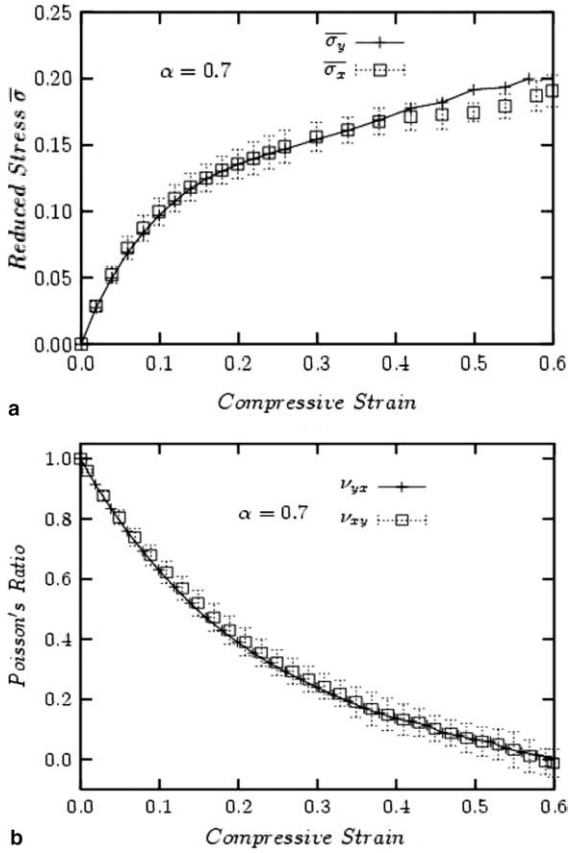

Fig. 3. (a) The mean reduced stress–strain predictions (from FEA), for honeycomb compression in either the x- or y-direction. In each case $\alpha = 0.7$ and $\rho = 0.01$. (b) The corresponding mean Poisson's ratio results.

are shown only for the results due to compression in the x-direction. Fig. 3a and b show that the mean predicted results for both the compressive stress and the Poisson's ratio are generally very close for the two orthogonal directions. Therefore, while results may vary considerably between individual random samples, the mean results exhibit a high level of isotropy with respect to both properties over much of the applied strain range.

3.5. The effect of varying cell regularity on the high-strain honeycomb properties

The effect of varying the cell irregularity parameter, α, on the stress–strain response is shown in Fig. 4. In each case the FEA results represent the mean of 10–20 successful runs (generated from 20 to 60 attempted runs as stated), and the relative density is fixed at 0.01. Fig. 4a–c show the mean simulated (FEA) compressive stress–strain responses for Voronoi honeycombs with α values of 0, 0.4 and 0.7, respectively, which are compared in each case with the predictions of Eq. (17) (see Section 4). In Fig. 4d and e the results with varying α are amalgamated for the simulated (FEA) and predicted (Eq. (17)) results respectively, and compared with the corresponding result for a periodic regular hexagonal honeycomb. The FEA results in Fig. 4d indicate that a highly irregular honeycomb has a larger tangential modulus at very low strains and supports a lower effective stress at high strains compared with a more regular honeycomb. The compressive

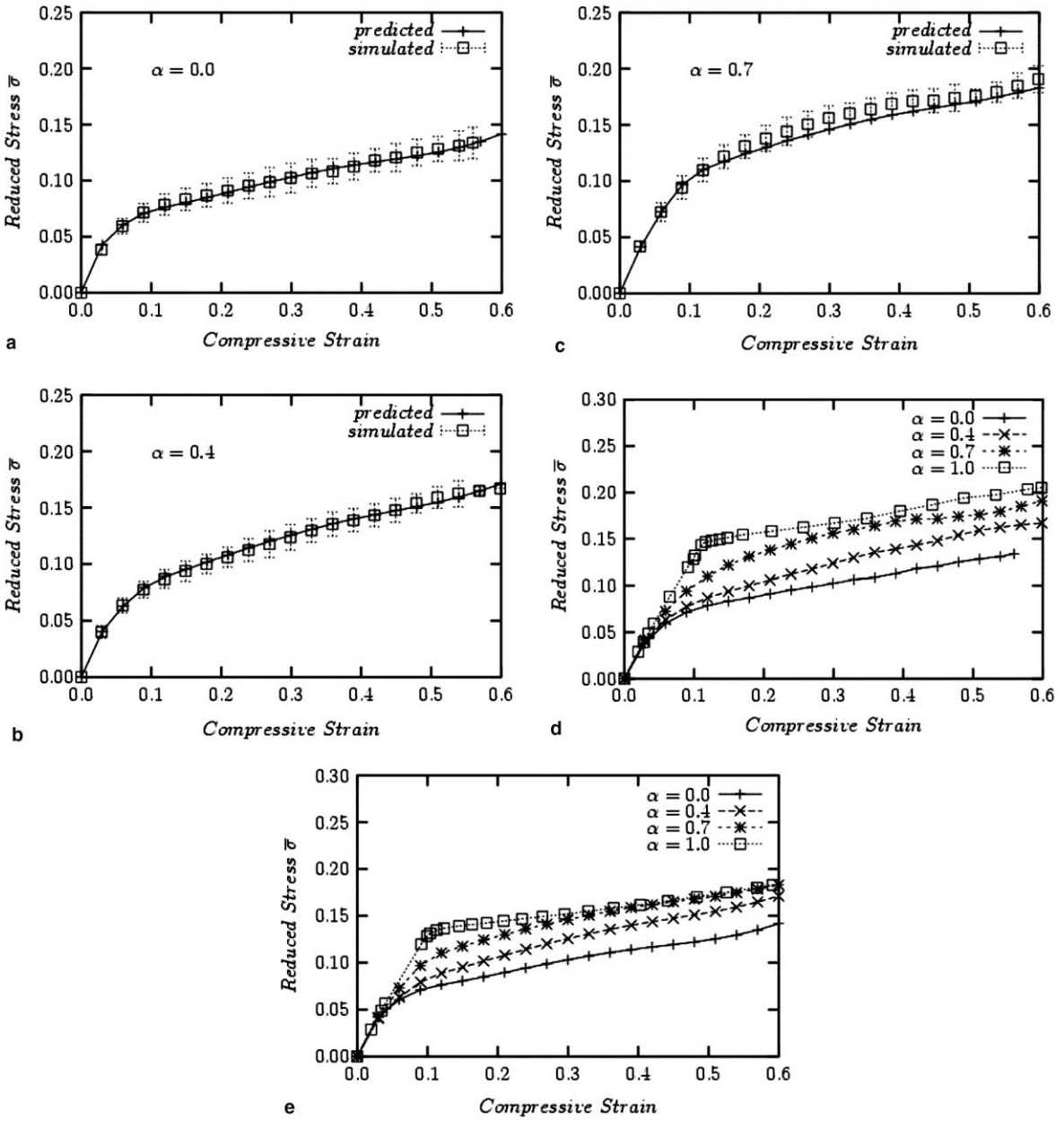

Fig. 4. The effect of cell irregularity on the mean reduced stress–strain relationships for Voronoi honeycombs, predicted using FEA and Eq. (17) for (a) $\alpha = 0.0$; (b) $\alpha = 0.4$; and (c) $\alpha = 0.7$. In (d) all FEA results; and in (e) all Eq. (17) results are compared with the regular ($\alpha = 1.0$) result.

strength of a honeycomb, defined as the maximum value of stress achieved during the simulated compression (Silva and Gibson, 1997), therefore decreases as the irregularity increases. Chen et al. (1999) and Silva and Gibson (1997) also found that an irregular honeycomb (a delta honeycomb) has a lower non-dimensional yield strength than a regular honeycomb. The effect of increasing irregularity on the Poisson's

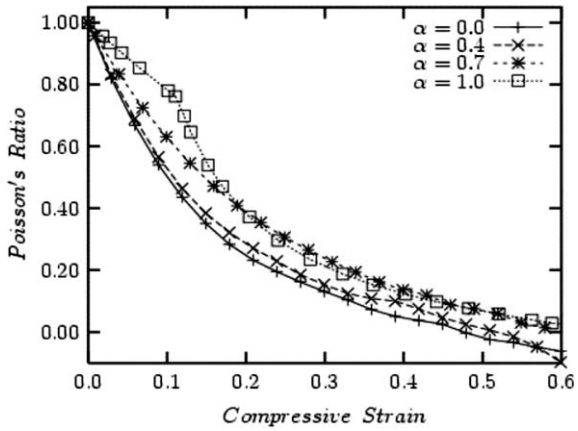

Fig. 5. The effect of cell irregularity on the mean Poisson's ratio results for Voronoi honeycombs, predicted using FEA for a range of values of α.

ratio of a Voronoi honeycomb is shown in Fig. 5 (in which the definition of the Poisson's ratio is applied to high strains). A progressive decrease in the Poisson's ratio is observed with increasing irregularity.

3.6. The effect of varying relative density

The honeycomb relative density, ρ, was defined in Eq. (3), and is set according to the (common) thicknesses of the cell walls. Figs. 6 and 7 show respectively the FEA predictions for compressive stress and Poisson's ratio in Voronoi honeycombs for which $\alpha = 0.7$ and the relative density is 0.01, 0.02, 0.04 or 0.08. It can be seen that the compressive stress and Poisson's ratio predictions are not highly affected by changes to ρ over the described range. Since it is expected that cell wall bending should be the dominant deformation at very low relative densities, it may be inferred from Figs. 6 and 7 that this continues to be the case up to relative densities of 0.08.

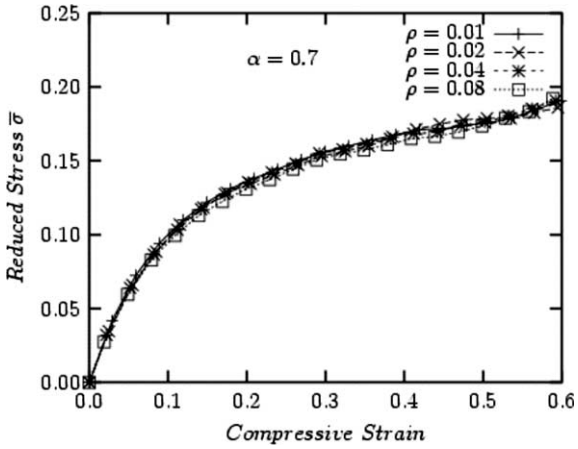

Fig. 6. The influence of relative density on the mean reduced stress–strain FEA predictions for Voronoi honeycombs with regularity parameter value $\alpha = 0.7$.

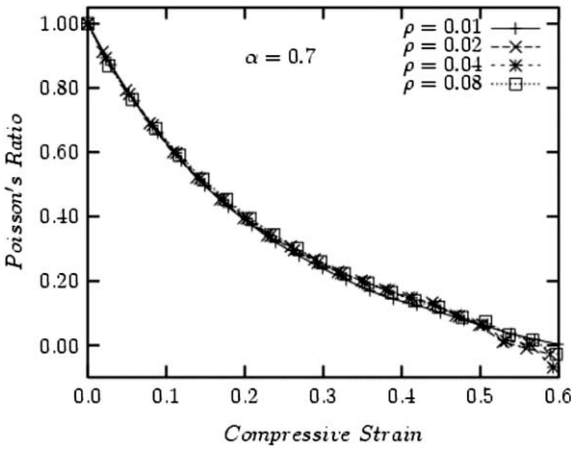

Fig. 7. The influence of relative density on the mean Poisson's ratio FEA predictions for Voronoi honeycombs with regularity parameter value $\alpha = 0.7$.

4. Analytic model

The theoretical high-strain deformation behaviour of a regular hexagonal honeycomb has been derived by Zhu and Mills (2000) for compression along two orthogonal axes which were labelled the x- and y-directions (the y-direction, unlike the former, is aligned with many of the cell walls in the undeformed structure). Below a compressive strain of about 0.10, the predicted stress for compression in the x-direction is lower than that for the y-direction and vice versa above this strain. In addition there is a well-defined plateau in the stress–strain response for y-direction compression, compared with a gradual softening of the curve for the x-direction. The reason for this difference is that, while there is no junction rotation during compression in the x-direction, there is a sudden marked rotation of the junctions at the onset of the plateau region which is referred to as 'elastic buckling'.[2] The curve of $\alpha = 1$ in Fig. 8 shows the relationship between the junction rotation and the compressive strain for a regular honeycomb during compression in the y-direction. Since localised cell buckling is a feature of the compression of an irregular Voronoi honeycomb at high strain (see Figs. 9 and 10 which show localised cell collapse, and Fig. 8 which indicates large-scale junction rotation), the theoretical stress–strain relationship for y-direction compression of a regular hexagonal honeycomb (Zhu and Mills, 2000) will be taken as the starting point of a model for the compression of a Voronoi honeycomb and is represented here by

$$\overline{\sigma_0} = f(\varepsilon) \tag{5}$$

or, alternatively:

$$\varepsilon = F(\overline{\sigma_0}) \tag{6}$$

Both Eqs. (5) and (6) describe the same reduced stress–strain relationship for a regular hexagonal honeycomb, which is shown as the central curve plotted in Fig. 11.

For an irregular Voronoi honeycomb, the low-strain Young's modulus has previously been predicted using a 'springs in parallel' model (Zhu et al., 2001a). In this model, the cells of the honeycomb were assumed to experience the same compressive strain but different compressive stresses. The values which were

[2] 'Elastic buckling' in the present work is taken to mean any sudden increase in the deformation rate of a cell wall or region in a honeycomb under a constant applied strain rate on the structure as a whole.

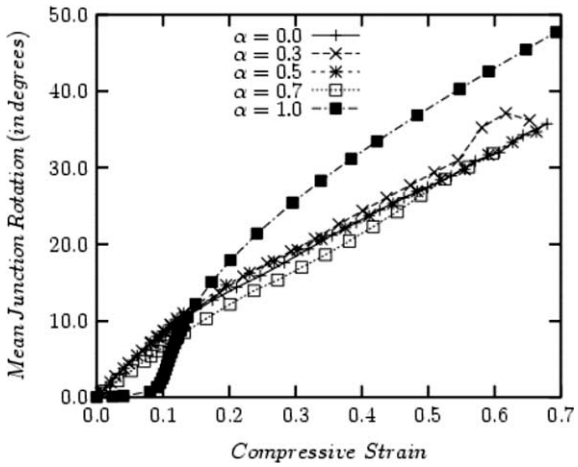

Fig. 8. The variation in the mean absolute junction rotation with compressive strain in Voronoi honeycombs of varying regularity (from FEA); also shown is the theoretical result for $\alpha = 1.0$.

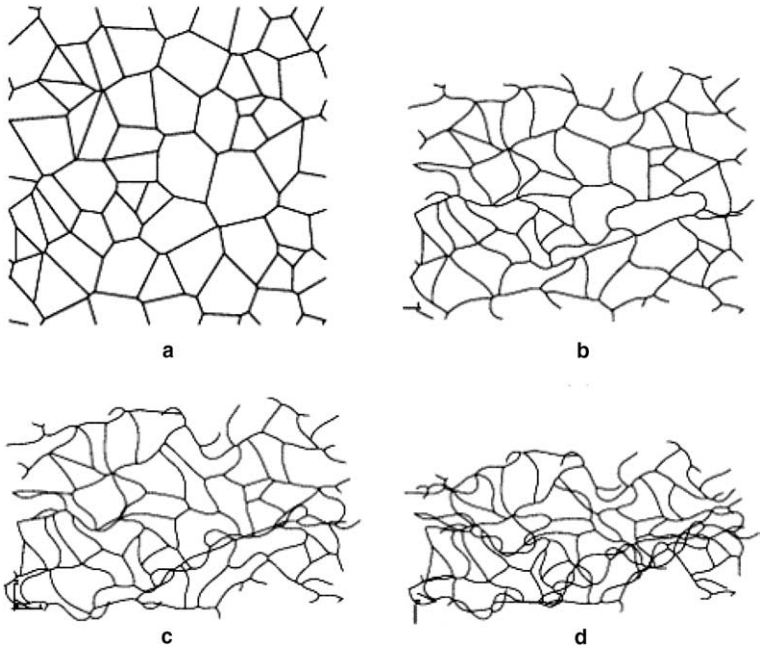

Fig. 9. The deformed structures, as predicted using FEA, of a random Voronoi honeycomb with $\alpha = 0.0$ at compressive strains of (a) $\varepsilon = 0.0$; (b) $\varepsilon = 0.24$; (c) $\varepsilon = 0.42$; and (d) $\varepsilon = 0.61$.

derived for the reduced Young's modulus $\overline{E}$ using this model (where $\overline{E} = E/E_s\rho^3$) are reproduced in Fig. 12, from which it is seen that the Young's modulus decreases with increasing regularity of the Voronoi honeycomb (note that the values plotted in Fig. 12 are *relative* to the reduced Young's modulus of the regular honeycomb). Thus, an irregular honeycomb is stiffer than the regular structure at low strains. Chen et al. (1999) and Silva et al. (1995) also found that an irregular honeycomb (a delta honeycomb, i.e.

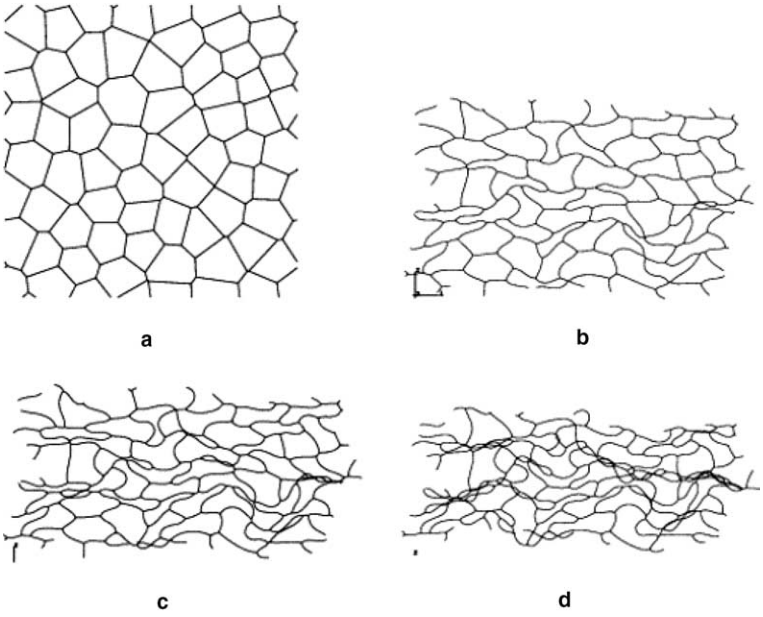

Fig. 10. The deformed structures, as predicted using FEA, of a random Voronoi honeycomb with $\alpha = 0.7$ at compressive strains of (a) $\varepsilon = 0.0$; (b) $\varepsilon = 0.36$; (c) $\varepsilon = 0.48$; and (d) $\varepsilon = 0.62$.

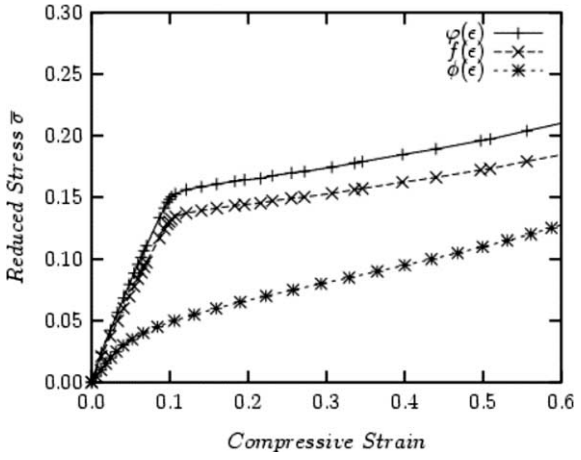

Fig. 11. The reduced compressive stress–strain relationship $f(\varepsilon)$ for a regular hexagonal honeycomb in the y-direction; also $\varphi(\varepsilon)$ and $\phi(\varepsilon)$ for Voronoi honeycombs with $\alpha = 0.4$.

$\alpha = 0.7$) has a non-dimensional Young's modulus about 5% larger than a regular honeycomb. If the 'springs in parallel' model were sufficient to describe the deformation of an irregular Voronoi honeycomb (that is, if all cells experienced approximately the same strain) then the reduced stress–strain relationship might be approximated by

$$\overline{\sigma_p} = \varphi(\varepsilon) = \frac{\overline{E}}{\overline{E}_R} f(\varepsilon) \tag{7}$$

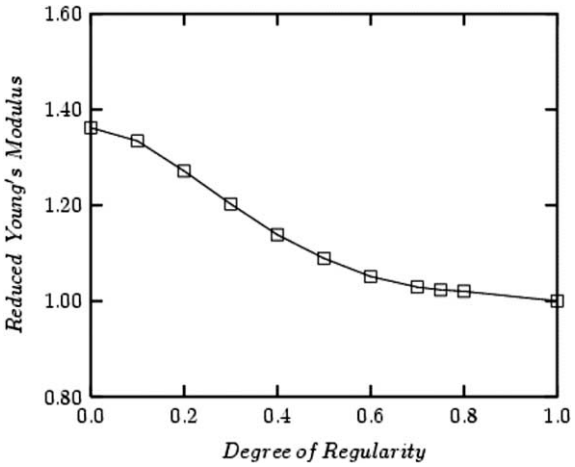

Fig. 12. The effect of cell irregularity on the relative reduced Young's modulus (to that of a regular hexagonal honeycomb) of Voronoi honeycombs with $\rho = 0.01$ (from Zhu et al., 2001a).

in which $\overline{E}$ is the reduced Young's modulus of an irregular honeycomb, and $\overline{E}_R$ is that of the regular hexagonal case. It describes a stiffer relationship than Eq. (5) because $\frac{\overline{E}}{\overline{E}_R}$ is larger than 1.0 when α is below 1.0 (see Fig. 12). For a Voronoi honeycomb with $\alpha = 0.4$, the relationship in Eq. (7) is represented by the upper of the three curves in Fig. 11.

In the compression of an irregular honeycomb, however, cell buckling has been seen to play an important role at high strains (see Figs. 9 and 10), and consequently an irregular honeycomb has a lower reduced stress than a more regular one in this region (see Fig. 4d). Hence, at high strains not all cells are compressed to the same extent and a 'springs in parallel' model is inappropriate. In order to describe buckling behaviour, a 'springs in series' model, in which all cells are assumed to experience the same compressive stress but different compressive strains, will now be developed.

For a single long and thin beam of uniform cross-section, the force, P, at which buckling occurs is given by

$$P = \frac{KE_sI}{l^2} \tag{8}$$

where E_s is the Young's modulus of the beam material, E_sI is the bending stiffness, l is the beam length, and K is a constant which depends upon the beam end constraints. Thus, for a low density regular hexagonal honeycomb, the reduced buckling stress can be expressed as:

$$\overline{\sigma_0} = \frac{\sigma_0}{E_s\rho^3} = \frac{c_1P}{A_0^{1/2}E_s\rho^3} = \frac{Ct_0^3}{l_0^2A_0^{1/2}\rho^3} \tag{9}$$

in which c_1 and C are (different) constants, A_0 is the area of each regular cell (in the xy-plane), t_0 is the common cell wall thickness, and l_0 the common cell wall length (note that the depth of the honeycomb in the z-direction is incorporated in constant c_1). For an irregular cell, the reduced buckling stress may similarly be expressed:

$$\overline{\sigma_i} = \frac{Ct_i^3}{l_i^2A_i^{1/2}\rho^3} \tag{10}$$

where $\overline{\sigma_i}$, t_i, l_i and A_i each refer to cell i, being respectively the reduced buckling stress, the cell wall thickness, the mean cell wall length, and the cell area; the constant C is assumed to be the same as that in Eq. (9).

Dividing Eq. (10) by Eq. (9) gives:

$$\overline{\sigma_i} = \frac{t_i^3 l_0^2}{t_0^3 l_i^2}\left(\frac{A_0}{A_i}\right)^{1/2}\overline{\sigma_0} \tag{11}$$

The area of a regular cell, A_0, is equal to the mean cell area for an irregular honeycomb with the same number of cells and t_i (which is set according to Eq. (3) to give a value of $\rho = 0.01$) is the thickness of all cell walls in the irregular honeycomb. The value of t_i is smaller than t_o if $\alpha \neq 1.0$ since an irregular Voronoi honeycomb has a mean cell wall length which is greater than l_0, while the mean number of cell walls per cell remains at 6.0 (Zhu et al., 2001b).

Since the stress for a regular hexagonal honeycomb, $\overline{\sigma_0}$, is a known function of the compressive strain (see Eq. (5) and Fig. 11), the above relation may be written:

$$\overline{\sigma_i} = \frac{t_i^3 l_0^2}{t_0^3 l_i^2}\left(\frac{A_0}{A_i}\right)^{1/2} f(\varepsilon_i) \tag{12}$$

or, alternatively, in terms of the strain:

$$\varepsilon_i = F\left(\frac{t_0^3}{t_i^3}\beta_i\overline{\sigma_i}\right) \tag{13}$$

in which $\overline{\sigma_i}$ and ε_i are respectively the reduced stress and compressive strain for cell i. The function F is the same as that in Eq. (6), but the variable is instead $\frac{t_0^3}{t_i^3}\beta_i\overline{\sigma_i}$. The ratio $\frac{t_0^3}{t_i^3}$ is constant for a given honeycomb and varies with the regularity parameter α, while β_i is given by

$$\beta_i = \frac{l_i^2}{l_0^2}\left(\frac{A_i}{A_0}\right)^{1/2} \tag{14}$$

If cell buckling were the only deformation mechanism present, then the reduced compressive stress for an individual cell, $\overline{\sigma_i}$, would be equal to the overall value for the honeycomb, $\overline{\sigma_s}$ (where the subscript refers to the 'springs in *series*' model). Consequently, the total compressive strain on the Voronoi honeycomb would be given by

$$\varepsilon = \sum_{i=1}^{n}\varepsilon_i P_A(\beta_i) = \sum_{i=1}^{n} F\left(\frac{t_0^3}{t_i^3}\beta_i\overline{\sigma_s}\right)P_A(\beta_i) \tag{15}$$

where $P_A(\beta_i)$ is the area probability (the proportion of total area occupied) of the cells in a Voronoi honeycomb with a parameter value of β_i. The cell area probability distributions, $P_A(\beta_i)$, have been obtained based upon statistical analysis of 10^5 cells in Voronoi honeycombs with different values for the regularity parameter, α, as shown in Fig. 13 (in which β_i are grouped in equal intervals of 0.1). When the strain on a particular cell, ε_i, reaches 0.95 it is assumed that the cell cannot be compressed any further, therefore the maximum value of $F(\frac{t_0^3}{t_i^3}\beta_i\overline{\sigma_s})$ in Eq. (15) is taken to be 0.95. For convenience, the relationship in Eq. (15) is represented in terms of the stress by

$$\overline{\sigma_s} = \phi(\varepsilon) \tag{16}$$

which is dependent upon the value of the regularity parameter α. For Voronoi honeycombs with $\alpha = 0.4$, this relationship is shown as the lower of the three curves in Fig. 11.

The simulated (FEA) results in Fig. 4e indicate that an irregular honeycomb has a larger tangential modulus at low strains than a more regular one, which is in agreement with the 'springs in parallel' model introduced in Zhu et al. (2001a). At higher strains, however, cell buckling dictates that the compressive stress decreases with increasing honeycomb irregularity, which is consistent with a 'springs in series' model. Thus,

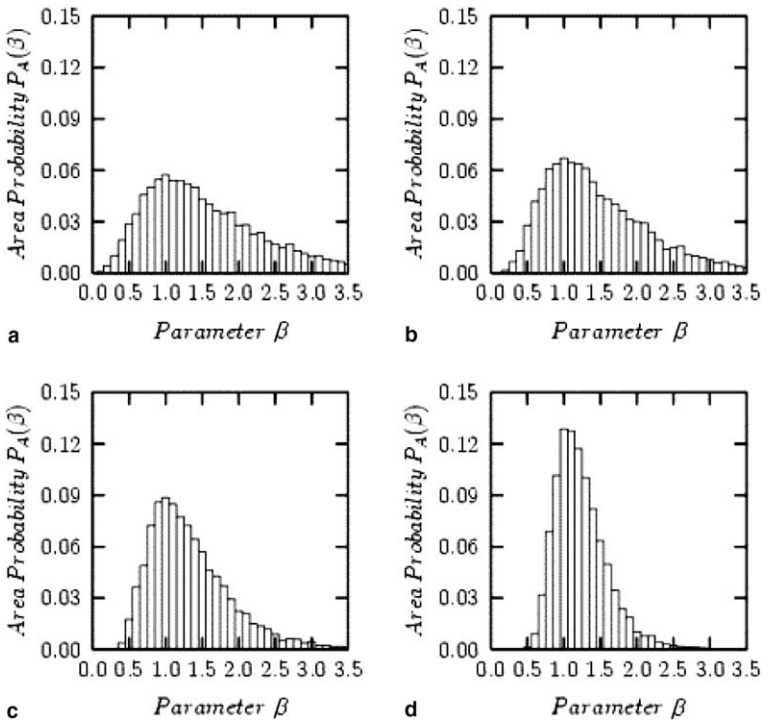

Fig. 13. The area probability distributions of cells with values of parameter β (see Eq. (14)) in random Voronoi honeycombs with: (a) $\alpha = 0.0$; (b) $\alpha = 0.3$; (c) $\alpha = 0.5$; and (d) $\alpha = 0.7$. The data is based upon 10^5 cells in each case, and is grouped in equal intervals of β of width 0.1.

both models are necessary in order to describe the stress–strain relationship over the entire strain range and Eqs. (7) and (16) are combined as follows:

$$\overline{\sigma^*} = G(\varepsilon) = [\varphi(\varepsilon)]^{1-\gamma}[\phi(\varepsilon)]^{\gamma} \tag{17}$$

where γ is the weight of the role played by the 'springs in series' model in the honeycomb deformation. The value of γ has been determined, by fitting Eq. (17) to the simulated results in Fig. 4a–c, to be given by

$$\gamma = 1 - e^{-18\varepsilon+60\varepsilon^2-70\varepsilon^3} - \varepsilon(1.6 - 3\varepsilon - 1.2\varepsilon^2 + 6\varepsilon^3 - 2\varepsilon^4) - \alpha\varepsilon(0.92 + 2.7\alpha + 0.6\varepsilon - 4.0\alpha\varepsilon) \tag{18}$$

When ε tends to zero γ also tends to zero, and the reduced Young's modulus (the initial tangential modulus) tends to the value predicted by the 'springs in parallel' model, $\overline{E}$, shown in Fig. 12; this is consistent with the previous results in the case of small deformation (Zhu et al., 2001a). Values of γ for increasing strain and α values of 0, 0.4 and 0.7 are given in Table 1; the highest values of γ (the role of 'cell buckling') are seen when α is small and ε is large. The presence of cell buckling (and hence the involvement of the 'springs in series' model) is associated with large junction rotation. A plot of the mean absolute junction rotation, as determined by FEA, with compressive strain is shown in Fig. 8, from which it can be seen that the junction rotations tend to zero when the compressive strain tends to zero. This suggests that the 'springs in parallel' mechanism does indeed dominate at low compressive strains.

The predictions of the combined model in Eq. (17) are shown up to a compressive strain of 0.6 in Fig. 4. There is good agreement between these predictions and those of the FEA runs for Voronoi honeycombs with varying degrees of regularity α, implying that the phenomenological model developed in this paper

Table 1
Values for γ, the 'springs in series' weighting in Eq. (17), for increasing values of the honeycomb strain ε and the regularity parameter α

ε	γ		
	$\alpha = 0.0$	$\alpha = 0.4$	$\alpha = 0.7$
0.00	0.0000	0.0000	0.0000
0.01	0.1441	0.1361	0.1245
0.02	0.2550	0.2391	0.2163
0.03	0.3408	0.3172	0.2832
0.04	0.4075	0.3761	0.3312
0.05	0.4594	0.4204	0.3649
0.10	0.5898	0.5138	0.4085
0.15	0.6240	0.5130	0.3636
0.20	0.6286	0.4846	0.2968
0.30	0.6276	0.4236	0.1761
0.40	0.6587	0.4027	0.1183
0.50	0.7236	0.4236	0.1251
0.60	0.7438	0.4078	0.1180

can be used to describe the compressive deformation of low density honeycombs. The more irregular the honeycomb structure (i.e. the smaller the parameter α), the more important is the role played by cell buckling and the 'springs in series' model at a fixed compressive strain. For a regular honeycomb ($\alpha = 1.0$), both functions $\varphi(\varepsilon)$ (Eq. (7)) and $\phi(\varepsilon)$ (Eq. (16)) reduce to $f(\varepsilon)$ (Eq. (5)) and hence Eq. (17) gives the correct result. The co-existence of both the 'springs in parallel' and 'springs in series' behaviours at high compressive strains is comparable to similar findings for the high strain compression of irregular open-cell 3D foams (Zhu and Windle, 2002).

5. Discussion

The applicability of the above results, both FEA and those predicted by Eq. (17), may be limited by two factors: one is that the maximum strain in the cell walls may exceed the yield strain of the solid material should elastomeric behaviour cease; another is that the cell walls may come into contact, or overlap, which is not taken into account. Both of these issues will now briefly be considered.

Since both the maximum bending strain developed in a honeycomb cell wall, $e_{\mathrm{b\,max}}$, and the honeycomb relative density, ρ, (see Eq. (3)) are directly proportional to the cell wall thickness, t, the ratio $e_{\mathrm{b\,max}}/\rho$ is a unique function of the honeycomb strain and an appropriate variable for investigating possible yielding in the honeycomb structure (Zhu and Mills, 2000). For low density honeycombs the axial strains in the cell walls are small in comparison with the bending strains, so that the maximum bending strain is taken as the yielding criterion. Fig. 14 shows the mean reduced maximum bending strain, $e_{\mathrm{b\,max}}/\rho$, taken across FEA results for five different Voronoi honeycombs for each value of α shown, as a function of the overall honeycomb strain. For comparison the theoretical result for a regular hexagonal honeycomb (Zhu and Mills, 2000) is also shown. Fig. 14 indicates that the higher the irregularity (i.e. the smaller is α), the larger will be the maximum bending strain developed in the cell walls. The results imply that if the relative density of a Voronoi honeycomb is 0.005 or smaller, then the maximum strain in the solid material will be less than 0.01 up to an overall honeycomb compressive strain of 0.6.

In terms of the yield stress, σ_{ys}, a well-known property of most materials, the maximum allowed (reduced) bending strain before yielding occurs may be written:

$$e_{\mathrm{b\,max}} \Big/ \rho = \frac{\sigma_{\mathrm{ys}}}{E_{\mathrm{s}}\rho} \tag{19}$$

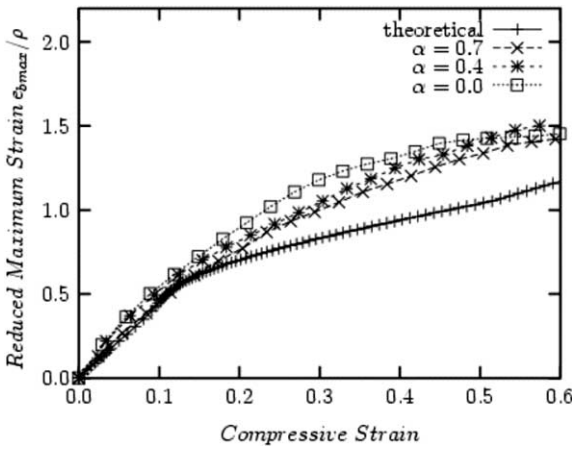

Fig. 14. The mean reduced maximum bending strain $e_{b\,max}/\rho$ (from FEA) in the cell walls of Voronoi honeycombs with $\alpha = 0.0$, 0.4 or 0.7; also shown is the theoretical $\alpha = 1.0$ result.

Therefore, given the yield stress and Young's modulus of the material, it can be determined by referring to Fig. 14 whether the material in a honeycomb of a given regularity is expected to yield by a particular compressive strain on the overall structure. Below the yield stress of the material there is no plastic deformation and (ignoring any viscoelastic behaviour in an elastomeric polymer) the predicted reduced stress–strain relationship of the honeycomb will be as shown in Fig. 4.

Silva and Gibson (Silva and Gibson, 1997) studied the compression of irregular Voronoi honeycombs using FEA and elastic-plastic cell wall elements. For a Voronoi honeycomb with a relative density of 0.015 and a σ_{ys}/E_s ratio of 0.01, which is an appropriate value for materials such as wood and bone (Reilly and Burstein, 1975), they obtained a honeycomb 'collapse strain' of 0.16 (see their Fig. 2d). From Eq. (19) and the values quoted above, the maximum reduced bending strain permitted in the cell walls of such a honeycomb before yielding occurs, $e_{b\,max}/\rho$, is 0.67. Therefore, by estimating the degree of irregularity from their Fig. 2a (α is approximately 0.7), the overall honeycomb strain at which yielding occurs may be determined from Fig. 14 to be 0.16, which agrees very well with their reported collapse strain. In addition, their stress–strain result is consistent in appearance with our own in Fig. 4c up to a compressive strain of 0.16.

We have also examined visually the deformed structures produced by the FEA simulations, examples of which are shown in Figs. 9 and 10 for Voronoi honeycombs with α values of 0.0 and 0.7, respectively. Fig. 9b represents the point at which cell walls first overlap, at an overall compressive strain of 0.24, in a fully-random ($\alpha = 0$) honeycomb. The strain at which cell walls came into contact generally increased with the value of α, and did not occur below a honeycomb compressive strain of 0.20 in the examples observed. In a more regular Voronoi honeycomb, for which $\alpha = 0.7$, cell wall contact occurred at a strain of 0.36 as shown in Fig. 10b; while in the case of a regular hexagonal honeycomb ($\alpha = 1.0$) this does not occur until the overall honeycomb strain is about 0.8 (Zhu and Mills, 2000). From Fig. 4d it can be seen that, regardless of the honeycomb regularity, there is an increase in compressive stress with compressive strain, and thus the honeycombs do not 'collapse' even when some of the cell walls overlap. It should be noted that, the solid material is treated as linear elastic throughout the deformation. Cell wall 'collapse' and 'contact' (Papka and Kyriakides, 1994, 1998) are caused more likely by material's non-linearity than by geometrical non-linearity. Therefore, the stress–strain relationships predicted in this paper are expected to apply to compressive strains up to cell wall contact, depending upon the honeycomb relative density.

Turning to the Poisson's ratio predictions, Fig. 5 shows that the mean Poisson's ratio generally decreases at a fixed compressive strain as the regularity of the honeycomb decreases. It can be seen that the Poisson's

ratio goes negative above a compressive strain of 0.47 in a fully-random ($\alpha = 0$) honeycomb, and negative above a compressive strain of 0.56 in a regular hexagonal ($\alpha = 1.0$) honeycomb; where large-scale junction rotations are responsible for this behaviour in each case. In the case of a regular honeycomb there is also a discontinuity in the gradient of the relationship between Poisson's ratio and compressive strain, caused by the onset of large-scale junction rotations at a compressive strain of 0.102 (which was described as a transition from the 'mode 1' to 'mode 2' deformation pattern in Zhu and Mills, 2000). The variation in the mean absolute junction rotation (in degrees) with compressive strain is shown in Fig. 8 for Voronoi honeycombs of varying regularity. Each curve in Fig. 8 represents an average over five samples, with the exception of the result for a regular hexagonal honeycomb which is plotted for comparison (Zhu and Mills, 2000). In general there is an approximately linear increase in the magnitude of the mean junction rotation in an irregular honeycomb as the compressive strain increases, and the degree of irregularity has little effect on the relationship. In the regular hexagonal case the dependency is rather different, there being little or no junction rotation up to a strain of 0.102 followed by a sudden increase at the onset of a concerted elastic buckling throughout the structure.

6. Conclusions

We have extended the previous low-strain analysis of the compression of irregular Voronoi honeycombs with periodic boundary conditions (Zhu et al., 2001a) to compressive strains of 0.6 for values of the regularity parameter, α, between 0 and 0.7. Finite element simulations have been carried out using the ABAQUS software, and all cell walls have been treated as straight elastic beams of uniform thickness; consequently our analysis is limited to honeycombs of low relative density (densities of 0.08 or lower have been used). The results indicate that a honeycomb with high geometric irregularity has a larger tangential modulus at low strain and sustains a lower compressive stress at high strain (above approximately 0.04) compared with a more regular honeycomb. The stress–strain response for y-direction compression of a regular hexagonal honeycomb (Zhu and Mills, 2000) may be taken as an upper bound for the mechanical properties of a honeycomb of the same relative density at high strain. The compression behaviour of a low density irregular honeycomb has also been modelled using a combination of 'springs in parallel' and 'springs in series' mechanisms. While the coexistence of both mechanisms is required in order to account for the observed stress–strain response, the 'springs in series' model becomes more important as the irregularity of the honeycomb and, in many cases, the compressive strain increases. The Poisson's ratio of an irregular honeycomb is observed to generally decrease as the compressive strain and the irregularity of the honeycomb increases. For honeycombs with an α value of 0.7, both the stress–strain response and the Poisson's ratio were affected little by the value of the relative density (densities of 0.08 and below were used) and the structures were, on average, approximately isotropic with respect to the orthogonal x- and y-directions. The mean junction rotation in an irregular honeycomb has been found to increase approximately linearly with the compressive strain, and is largely unaffected by the degree of irregularity. Finally, the dependency of the maximum cell wall bending strain upon the overall honeycomb strain has been evaluated for honeycombs of varying regularity; this enables the overall strain to be predicted at which yielding of the cell wall material of such a honeycomb is likely to occur.

Acknowledgments

The authors wish to thank Drs. Anthony Cunningham and John Hobdell of Huntsman Corporation for their continued support of, and intellectual contributions to this work. They also wish to acknowledge the

University of Cambridge for the use of their SGI High Performance Computing Facility Origin 2000 computer and associated staff time.

References

Abd El-Sayed, F.K., Jones, R., Burgess, I.W., 1979. A theoretical approach to the deformation of honeycomb based composite materials. Composites 10, 209–214.

Chen, C., Lu, T.J., Fleck, N.A., 1999. Effect of imperfections on the yielding of two-dimensional foams. J. Mech. Phys. Solids 47, 2235–2272.

Gibson, L.J., Ashby, M.F., 1997. Cellular Solids: Structure and Properties, second ed. Cambridge University Press, Cambridge, UK.

Gibson, L.J., Ashby, M.F., Schajer, G.S., Robertson, C.I., 1982. The mechanics of two-dimensional cellular materials. Proc. Roy. Soc. Lond. A 382, 25–42.

Masters, I.G., Evans, K.E., 1996. Models for the elastic deformation of honeycombs. Compos. Struct. 35, 403–422.

Papka, S., Kyriakides, S., 1994. In-plane compressive response and crushing of honeycomb. J. Mech. Phys. Solids 42, 1499–1532.

Papka, S.D., Kyriakides, S., 1998. Experiments and full-scale numerical simulations of in plane crushing of a honeycomb. Acta Mater. 46, 2765–2776.

Reilly, D.T., Burstein, A.H., 1975. The elastic and ultimate properties of compact bone tissue. J. Biomech. 8, 393–405.

Silva, M.J., Gibson, L.J., 1997. The effects of non-periodic microstructure and defects on the compressive strength of two-dimensional cellular solids. Int. J. Mech. Sci. 39, 549–563.

Silva, M.J., Hayes, W.C., Gibson, L.J., 1995. The effects of non-periodic microstructure on the elastic properties of two-dimensional cellular solids. Int. J. Mech. Sci. 37, 1161–1177.

Warren, W.E., Kraynik, A.M., 1987. Foam mechanics: the linear elastic response of two-dimensional spatially periodic cellular materials. Mech. Mater. 6, 27–37.

Zhu, H.X., Hobdell, J.R., Windle, A.H., 2001a. Effects of cell irregularity on the elastic properties of 2D Voronoi honeycombs. J. Mech. Phys. Solids 49, 857–870.

Zhu, H.X., Mills, N.J., 2000. The in-plane non-linear compression of regular honeycombs. Int. J. Solids Struct. 37, 1931–1949.

Zhu, H.X., Thorpe, S.M., Windle, A.H., 2001b. The geometrical properties of irregular two-dimensional Voronoi tessellations. Phil. Mag. A 81, 2765–2783.

Zhu, H.X., Windle, A.H., 2002. Effects of cell irregularity on the high strain compression of open-cell foams. Acta Mater. 50, 1041–1052.